

1 **Heterodi- (Fe, Pd/Pt) and Heterotrimetallic (Fe₂, Pd) Complexes Derived from 4-**
2 **(Ferrocenylmethyl)-N-(2-methoxyethyl)-3,5-diphenylpyrazole as Potential Antitumoral Agents**

3
4
5
6
7
8 Eva Guillén^[a] Asensio González^[b] Concepción López^{*[a]} Pradipta K. Basu^[a,c] Amrita Ghosh^[c]
9 Mercè Font-Bardía,^[d] Carme Calvis,^[e] and Ramón Messeguer^[e]

10
11
12
13
14
15
16
17
18
19
20
21 [a] Departament de Química Inorgànica, Facultat de Química, Universitat de Barcelona, Martí I
22 Franquès 1–11, 08028 Barcelona, Spain

23 E-mail: conchi.lopez@qi.ub.es

24 http://www.ub.edu/inorgani/ca/recerca_qbo.html

25 [b] Laboratory de Química Orgànica, Facultat de Farmàcia, Universitat de Barcelona, Pl. Pius XII s/n,
26 08028 Barcelona, Spain

27 [c] Department of Chemistry, Durgapur Government College, Durgapur, Burdwan 713214, India

28 [d] Unitat de Difracció de raig-X, Centre Científic I Tecnològic, Universitat de Barcelona, Solé i Sabaris
29 1–3, 08028 Barcelona, Spain

30 [e] Biomed Division, LEITAT Technological Center, Parc Científic de Barcelona, Edifici Hèlix, C/
31 Baldri I Reixach 13–21, 08028 Barcelona, Spain

32
33
34
35

36 **ABSTRACT:**

37

38 The study of the reactivity of the pyrazole derivative 1-[MeO-(CH₂)₂]-3,5-Ph₂-4-(CH₂Fc)-(C₃N₂) (1,
39 Fc = ferrocenyl) with Na₂[PdCl₄], Pd(OAc)₂, and [MCl₂(dmsO)₂] (M = Pd or Pt, dmsO = dimethyl
40 sulfoxide) has allowed us to isolate trans-[Pd{κ-N-(1-{MeO(CH₂)₂}-3,5-Ph₂-4-{CH₂Fc}-
41 {C₃N₂})}Cl₂] (2), [Pd{κ²-C,N(1-{MeO(CH₂)₂}-3-{C₆H₄}-5-Ph-{C₃N₂})} {κ-N-(1-{MeO(CH₂)₂}-
42 3,5-Ph₂-4-{CH₂Fc}-{C₃N₂})}Cl] (3), [Pd{κ²-C,N(1-{MeO(CH₂)₂}-3-{C₆H₄}-4-{CH₂Fc}-5-Ph-
43 {C₃N₂})}Cl-(PPh₃)] (4), and the trans (5) and cis (6) isomers of [Pt{κ-N-(1-{MeO(CH₂)₂}-3,5-Ph₂-4-
44 {CH₂Fc}-{C₃N₂})}Cl₂(dmsO)]. Compound 1 acts as a N (in 2, 5, and 6) or (C,N)- donor ligand (in 4)
45 and shows both binding modes in 3. The cytotoxic assessment of 1–6 against MCF7, MDA-MB231
46 (breast), and HCT-116 (colon) cancer cell lines reveal that (1) 1 is more potent than 1-[MeO(CH₂)₂]-
47 3,5-Ph₂-(C₃H₅N₂) (V), (2) 2–6 have cytotoxic activity, (3) 2 and 3 are less active than 4–6, and (4) 6 is
48 the most potent compound against the three cancer cell lines.

49

50 INTRODUCTION

51

52 Pyrazole derivatives are valuable cores for the design and synthesis of compounds with interesting
53 applications in different fields, such as catalysis, agrochemistry, supra- and macromolecular chemistry,
54 as well as biomedicine.[1] Compounds of this type with outstanding anticancer, antiviral, antimicrobial,
55 antiglycemic, or even antiallergenic activities have been described.[2–5] Moreover, pyrazoles are useful
56 ligands in coordination and organometallic chemistry.[6] The nature and position of the substituents on
57 the ring, the metal ion (its oxidation number and environment), and even the ancillary ligands (donor
58 atoms, electron-donor ability, bulk, and relative orientation in the complex) modify the properties and
59 activities of the complexes.[7] Among the wide variety of transition metal complexes derived from
60 pyrazole, those containing PdII or PtII ions are probably the most attractive mainly owing to their
61 potential biological activity.[8,9] Compounds of this kind with greater antitumor activity and lower
62 toxicity than cis-[PtCl₂(NH₃)₂] (cisplatin) or antibacterial activity have been reported.[8,9]

63 On the other hand, bioorganometallic chemistry is a fast developing area of increasing interest, and the
64 idea of using organometallic complexes in drug discovery is becoming more and more popular.[10–12]
65 Antimalarials, antibacterials, and neuroprotectors based on organometallic compounds have been
66 described.[10,11] In this context, ferrocene derivatives are probably among those with the best
67 prospects.[13–15] One of the most promising strategies used to achieve new therapeutic agents consists
68 of the incorporation of a ferrocenyl (Fc) unit on the scaffold of a biologically active molecule.[10–15]
69 Commonly, this change increases the biological activity of the molecule and widens its range of
70 application. Owing to the increasing interest in pyrazole derivatives and new ferrocene-based drugs or
71 prodrugs, several groups have centered their attention on the design and synthesis of mixed ferrocenyl–
72 pyrazole derivatives.[16] Unfortunately, studies on their coordination ability to PdII or Previous studies
73 on the cytotoxic activities of pyrazoles 1-R₁-3,5-(R₂)₂-(C₃H₄N₂) (types IV and V in Figure 1) and their
74 PdII or PtII complexes against MCF7 and MDAMB231 breast cancer cell lines have shown that
75 compounds with R₂ = H or Me are less active than those with R₂ = Ph.[9b] Moreover, the replacement
76 of the Me₂N(CH₂)₂ [9b] group by a MeO(CH₂)₂ unit increases their cytotoxic activity.[9a] In view of
77 these findings and the increasing interest in new ferrocene derivatives with bioactive moieties, now we
78 present the hybrid Fc/pyrazole 1-[MeO(CH₂)₂]-3,5-Ph₂-4-(CH₂Fc)-(C₃N₂) (1, Figure 1) and report its
79 utility as a ligand for the synthesis of heterodi- or heterotrimetallic complexes containing FeII and PtII
80 or PdII ions and a study of the antitumoral activity of the compounds against breast (MDA-MB231 and
81 MCF7) and colon (HCT-116) cancer cell lines.

82

83 RESULTS AND DISCUSSION

84

85 Synthesis and Characterization of Ligand 1 Ligand 1 was prepared in good yield (80%) by the alkylation
86 of 3,5-Ph2-4-(CH2Fc)-(C3HN2) (IIa)[18] with 2-chloroethyl methyl ether (Scheme 1) by using the
87 same procedure as that described for indigo[19] or the N-methylated derivative 1-Me-3,5-Ph2-4-
88 (CH2Fc)-(C3N2).[18]

89 Compound 1 is a stable yellow solid at 298 K and exhibits high solubility in CH2Cl2, CHCl3, and
90 acetone. The characterization data (Supporting Information) agreed with the proposed formula, and
91 NMR spectroscopy studies confirmed the presence of the MeO(CH2)2 unit attached to the nitrogen
92 atom of the pyrazole ring.

93

94 Palladium(II) Complexes

95 In a first attempt to evaluate the potential coordination abilities of 1 to PdII ions, its reactivity with
96 Na2[PdCl4], [PdCl2(dmsO)2] (dmsO = dimethyl sulfoxide), and Pd(OAc)2 was studied under different
97 experimental conditions (Table 1, Entries 1–3; Scheme 2).

98 The treatment of 1 with Na2[PdCl4] (molar ratios 1:1 or 1:2) in MeOH at 298 K gave a yellow solid
99 (Table 1, Entry 1; Scheme 2, Step A). Its characterization data (Supporting Information) agreed with
100 those expected for the heterotrimetallic product 2, and its crystal structure confirmed the presence of
101 [Pd{κ-N-(1-{MeO(CH2)2}-3,5-Ph2-4-{CH2Fc}-{C3N2})}2Cl2] (Figure 2).

102 The PdII ion is located on an inversion center and, consequently, the relative disposition of the two
103 identical ligands is trans. The Pd–Cl bond length [2.3013(17) Å] is similar to those reported for most
104 trans-[Pd(κ-N-1-R1-3,5-Ph2-pyrazole) 2Cl2] complexes[9a,20,21] and its analogue Va [Figure 1; Pd1–
105 Cl1 2.3044(5) Å].[9a] The Pd–N1 bond length [2.007(4) Å] is slightly shorter than that in Va [Pd1–N1
106 2.020(19) Å] but only by an insignificant amount.[9a] The Pd1···H5 separation of 2.9 Å suggests a
107 weak agostic interaction.[22] The pyrazolyl rings are planar and nearly orthogonal to the “PdCl2” unit.
108 The phenyl rings form angles of 53.3 and 58.9° with the heterocycle. In the crystal, the molecules are
109 assembled through C–H···π intermolecular contacts[23] involving the H24 atom and the C5H5 ring (the
110 separation between H24 and the centroid of the C1–C5 ring is 2.604 Å).

111 Compound 2 was also isolated from the reaction of ligand 1 and [PdCl2(dmsO)2] (in molar ratios of 1:1
112 or 2:1) in MeOH under reflux (Table 1, Entry 2; Scheme 2, Step A). It should be noted that no evidence
113 of the formation of PdII complexes with a Pd–OMe bond or arising from the cyclometalation of any of
114 the rings was detected when Na2[PdCl4] or [PdCl2(dmsO)2] was used (Table 1, Entries 1 and 2).

115 As (1) cyclopalladated complexes are attracting great interest in a wide variety of areas,[24,25]
116 especially in view of their potential biological activity as cytotoxic, antimalarial, and antioxidants
117 agents,[25a,26,27] and (2) Pd(OAc)2 is a more potent metallating agent than Na2[PdCl4] or
118 [PdCl2(dmsO)2],[17,26,29] we also studied the reactivity of 1 with Pd(OAc)2. When equimolar amounts
119 of Pd(OAc)2 and 1 were heated to reflux in toluene for 24 h, the formation of Pd0 was detected on the
120 walls of the flask. Subsequent filtration through a Celite pad followed by column chromatography gave a
121 brownish solid (3; Table 1, Entry 3; Scheme 2, Step B).

122 The IR spectrum of 3 exhibited the typical bands for a monodentate OAc– ligand.[28] The 1H NMR
123 spectrum of 3 showed two sets of superimposed signals with relative intensities 1:1 and, thus, suggested
124 the presence of two different and inequivalent units of ligand 1. Moreover, in one of the sets of
125 resonances, the signals for 3a-H and 4a-H of the phenyl ring at the 3-position of the pyrazole ring
126 appeared high-field shifted in relation to the signals of the free ligand and to those of 2. This trend, also

127 observed for the cyclopalladated compounds derived from V,[9a] is typical of palladacycles containing
128 bidentate [C(sp², phenyl), N]- ligands.[30,31] These findings suggested one of the units of 1 adopted
129 this binding mode in 3, whereas the other acted as a N donor.

130 To confirm this hypothesis, further reactivity studies were performed. The treatment of 3 with LiCl first
131 and then an equimolar amount of PPh₃ gave a deep brown solid after concentration of the reaction
132 solution (Table 1, Entry 4; Scheme 2, Step C). The TLC and ¹H NMR spectrum of the raw material
133 revealed the presence of the free ligand (1) and a new PdII complex (4). The two products (1 and 4)
134 were separated in a molar ratio of ca. 1:1 by SiO₂ column chromatography. The elemental analysis and
135 mass spectrum of 4 (Supporting Information) agreed with those expected for [Pd{κ²-C,N-(1-
136 {MeO(CH₂)₂}-3-{C₆H₄}-4-{CH₂Fc}-5-Ph-{C₃N₂})}Cl(PPh₃)] (Scheme 2, Step C), in which the
137 PPh₃ ligand is in a cis arrangement to the metallated carbon atom.[32] The position of the singlet in the
138 ³¹P{¹H} NMR spectrum of 4 (δ = 43.6 ppm) is very similar to that of [Pd{κ²-C,N-(1-{MeO(CH₂)₂}-3-
139 {C₆H₄}-5-Ph-{C₃N₂})}Cl(PPh₃)] [9a] and falls in the range reported for other palladacycles with
140 “Pd{C(sp² phenyl),N}Cl(PPh₃)” cores.[17,18,26,29]

141

142 **Platinum(II) Complexes**

143 To compare the effect produced by the binding of the MII atom to ligand 1, we also studied the
144 reactivity of 1 with cis-[PtCl₂(dmsO)₂][33] under different experimental conditions (Table 1, Entries 5
145 and 6). The treatment of these two reagents (in molar ratios 1/PtII = 1 or 2) in MeOH under reflux for 1
146 h followed by the partial evaporation of the solvent gave a yellow solid (Table 1, Entry 5; Scheme 2,
147 Step D), which was identified as trans-[Pt{κ-N-(1-{MeO(CH₂)₂}-3,5-Ph₂-4-{CH₂Fc}-
148 {C₃N₂})}Cl₂(dmsO)] (5). These results are different from those obtained with [PdCl₂(dmsO)₂] (Table 1,
149 Entry 2), which gave the heterotrimetallic complex 2.

150 In view of the increasing interest in the cytotoxic activities of the trans and cis isomers of PtII
151 complexes containing mono- (L) or bidentate (L,L) N-donor ligands,[34,35] we also attempted the
152 preparation of the cis isomer of 5. Several strategies were used to achieve this aim. In a first attempt, the
153 reaction period (t) was increased gradually from 1 to 72 h. Under these experimental conditions, two
154 products were isolated by SiO₂ column chromatography. The major component was the trans isomer
155 (5); the characterization data of the minor product (6) agreed with those expected for cis-[Pt{κ-N-(1-
156 {MeO(CH₂)₂}-3,5-Ph₂-4-{CH₂Fc}-{C₃N₂})}Cl₂(dmsO)] (Scheme 1, Step E), and its crystal structure
157 (see below) confirmed this result. These two isomers were isolated in a 5/6 molar ratio of 1.0:0.65, but
158 larger reaction periods did not produce significant variations in their relative abundance (for t = 72 h, the
159 5/6 molar ratio was 1.0:0.70).

160 When the reaction was performed in the presence of NaOAc (molar ratio OAc-/PtII = 2) and in a
161 toluene/MeOH mixture (5:1) under reflux for 24 h, the 5/6 molar ratio decreased (Table 1, Entry 6), and
162 the cis isomer (6) became the major product.

163 Isomers 5 and 6 were separated by SiO₂ column chromatography and characterized by elemental
164 analysis, mass spectrometry, IR spectroscopy, and NMR spectroscopy (Supporting Information). Their
165 ¹H NMR spectra showed (1) one (for 5) or two singlets (for 6) of identical intensity for the protons of
166 the dmsO ligand and (2) two well-resolved triplets (for 5) or four multiplets (for 6) for the -(CH₂)₂-
167 protons of the pendant arm. The ¹⁹⁵Pt{¹H} NMR spectra showed a singlet in both cases, and the
168 chemical shifts were consistent with those of PtII compounds with a “N,Cl₂,S(dmsO)” set of donor
169 atoms. The magnitude of the shift [Δδ = δ(6) - δ(5) = 123 ppm] is similar to those reported for related
170 cis and trans isomers of PtII compounds with “Pt(N-donor ligand)Cl₂(dmsO)” cores.[17,27a,36]

171 The slow evaporation of a CH₂Cl₂ solution of 6 layered with MeOH at 298 K produced crystals suitable
172 for X-ray diffraction. The crystal structure confirmed the existence of [Pt{κ-N-(1-{MeO(CH₂)₂}-3,5-

173 Ph₂-4-{CH₂Fc}-{C₃N₂}}Cl₂-(dmsO)] (6), CH₂Cl₂, and MeOH molecules in a 1:1:1 ratio. In the
174 heterodimetallic molecules of 6 (Figure 3), the PtII atom is bound to nitrogen atom N1 of the pyrazolyl
175 unit, the sulfur atom S1 of the dmsO ligand, and two Cl- ligands (Cl1 and Cl2) in a cis arrangement
176 [Cl1-Pt-Cl2 bond angle: 89.86(5)°]. The bond lengths and angles around the PtII center are similar to
177 those of cis-[Pt{κ-N-1-(CH₂Fc)-3,5-Ph₂-(C₃H_N2)}Cl₂(dmsO)], which contains pyrazole I as a N-donor
178 ligand.[17a]

179 The three rings of the “3,5-Ph₂-C₃N₂” backbone are planar. The main plane of the heterocycle forms an
180 angle of ca. 74.01° with the coordination plane of the PtII ion, and the phenyl rings (C15-C20 and C21-
181 C26) are not coplanar with the pyrazole ring (the angles between the main planes are 66.9 and 63.6°).
182 The orientation of these two phenyl rings allows intramolecular C-H···π interactions between (1) the
183 C9-H9 bond of the C₅H₄ ring and the C21-C26 phenyl ring and (2) the other phenyl ring and the
184 hydrogen atom (H30) of the dmsO ligand.

185 In the crystal, the separation between the centroids of the cyclopentadienyl (Cp) ring of a molecule at (x,
186 y, z) and the C₅H₄ ring of a proximal unit is 3.295 Å, which indicate the existence of π-π stacking.
187 Moreover, two of the hydrogen atoms of the OMe unit (H29A and H29B) are involved in intermolecular
188 C-H···π interactions with the substituted ring of the Fc group and the pyrazolyl unit, respectively, of
189 another molecule at (1/2 - x, 1/2 - y, 1 - z).

190

191 Study of Cytotoxic Activities

192 In a first stage, two human breast cancer cell lines (MCF7 and MDA-MB231) were used to test the
193 cytotoxic activity of ligand 1 and complexes 2-6. Cisplatin (as a positive control) was also evaluated
194 under the same experimental conditions. A summary of the results obtained for the inhibition
195 concentrations (IC₅₀ in μm) of ligand 1, pyrazoles IV and V (Figure 1), and complexes 2-6 is presented
196 in Table 2. For comparison, the data for related PdII complexes derived from V are also included.

197 Ligand 1 exhibited outstanding activity (IC₅₀ 5.8 μm, greater than that of cisplatin) against these two
198 breast cancer cell lines. A comparison of the data presented in Table 2 for 1 and IV allows us to
199 conclude that the replacement of the hydrogen atom at the 4-position of the pyrazole ring (in IV) by the
200 -CH₂Fc unit to give 1 enhances the cytotoxic activity against these two (MCF7 and MDA-MB231) cell
201 lines. Moreover, as shown in Figure 4, the framework and substitution pattern of the pyrazole has a great
202 influence on its cytotoxic activity. For the studied pyrazoles 1, IV, and V, the cytotoxicity increases in
203 the order V > IV > cisplatin > 1 (against MCF7 and MDA-MB231 cell lines)

204 To evaluate the effect produced by the binding of the PdII or PtII atoms to the ligand, we also
205 investigated the cytotoxic activity of the new complexes against these cancer cell lines. The new PdII
206 complexes 2-4 exhibit cytotoxic activity (Figure 5 and Table 2) but are less active than the free ligand 1.
207 However, in general, they are more potent than their analogues derived from V. This suggests once more
208 that the -CH₂Fc group at the 4-position of the pyrazole ring increases their activity.

209 Better results were obtained for the trans (5) and cis (6) isomers of: [Pt{κ-N-(1-{MeO(CH₂)₂}-3,5-Ph₂-
210 4-{CH₂Fc}-{C₃N₂}}Cl₂(dmsO)]. These compounds exhibited outstanding activity (IC₅₀ 8.3 μm)
211 against the MCF7 and in the MDA-MB231 breast cancer cell lines. The cytotoxic activities increase
212 according to sequences:

213 3 < 2 < 4 < cisplatin < 5 < 6 (for MCF7 cell line)

214 3 < 2 < 4 < 5 < cisplatin < 6 (for MDA-MB231 cell line)

215 These trends are practically identical except for the position of cisplatin and reveal that the
216 heterotrimetallic compounds 2 and 3 are less potent than the heterodimetallic derivatives 4-6.

217 In view of the outstanding results obtained for some of the new products against the two breast cancer
218 cell lines, we decided to study their effect on the cisplatin-resistant HCT-116 colon cell line. A
219 comparison of the data (Table 2 and Figure 5) shows that their cytotoxic activity against this cell line
220 increases as follows:

221 $3 \leq 4 < 2 < 5 < \text{cisplatin} < 1 < 6$

222 Among the new products prepared in this work, complex 6 and the free ligand 1 are the most active
223 ones. Their potency against the HCT-116 cell line is greater (10 and 14 times, respectively) than that of
224 cisplatin under identical conditions.

225

226 **CONCLUSIONS**

227

228 The new hybrid ferrocenyl-pyrazole derivative 1-[MeO-(CH₂)₂]-3,5-Ph₂-4-(CH₂Fc)-(C₃N₂) (1) has
229 been prepared. The study of its reactivity with different PdII and PtII salts and complexes allowed us to
230 isolate and characterize three PdII compounds 2–4 and the trans (5) and cis (6) isomers of [Pt{κ-N-(1-
231 {MeO(CH₂)₂}-3,5-Ph₂-4-{CH₂Fc}-{C₃N₂})}Cl₂(dmsO)]. We have also proved that 1 is a versatile
232 and valuable ligand. It may (1) adopt two different binding modes {N donor (in 2, 5, and 6), [C(sp²,
233 phenyl), N]- (in 3), or even both simultaneously in the same complex (4)} and (2) produce heterotri- (2
234 and 3) or heterodimetallic complexes 4–6.

235 The new products 1–6 exhibit growth inhibitory activity against breast (MDA-MB231 and MCF7) and
236 colon (HCT-116) human cancer cell lines. We have also demonstrated that the presence of the CH₂Fc
237 moiety at the 4-position of the pyrazole ring plays a key role in determining the activity of the products.
238 Against the three cell lines, the PdII complexes 2 and 3 are less potent than the PtII derivatives 5 and 6
239 and the free ligand 1. Complex 6 is clearly more active than its trans isomer (5) against the three cell
240 lines assayed.

241 The free ligand and the cis isomer of [Pt{κ-N-(1-{MeO(CH₂)₂}-3,5-Ph₂-{C₃N₂}-4-{CH₂Fc}-
242 {C₃N₂})}Cl₂-(dmsO)] (6) are the most potent against the three cell lines. Their activities against the
243 cisplatin-resistant colon cell line (HCT-116) are especially relevant [ca. 10 (for 1) and 14 (for 6) times
244 bigger than that of cisplatin].

245 Although 6 has a slightly greater inhibitory effect than 1 against the cell lines MDA-MB231 and
246 HCT116, the new ligand is particularly attractive because it does not contain PtII and consequently
247 might not produce the typical and undesirable side effects of conventional PtII-based drugs. Thus,
248 among the new products presented here, compounds 1 and 6 appear to be excellent candidates for
249 further studies mainly centered on (1) the study of their cytotoxic activities against other cancer cell
250 lines (i.e., lung, ovarian, etc.), (2) the investigation of their effect on normal nontumor cells (i.e.,
251 fibroblasts), (3) additional studies (cell cycle arrest, induction of apoptosis, etc.) to gain further insights
252 into their mechanism of action, and (4) additional studies on their potential utility in combined therapies.
253 Preliminary studies in these fields are underway.

254

255 **EXPERIMENTAL SECTION**

256

257 **Materials and Methods:** 3,5-Ph₂-4-(CH₂Fc)-(C₃H_N₂), Na₂[PdCl₄], and complexes [MCl₂(dmsO)₂]
258 (M = Pd or Pt) were prepared as described previously,[17,31,36–38] and the remaining reagents were
259 obtained from commercial sources and used as received. The success of the synthesis of the PtII
260 complexes (5 and 6) is strongly dependent on the quality of the methanol; the presence of water results
261 in the formation of metallic platinum, other undesirable minor byproducts, and a significant decrease in
262 the yield. Thus, the use of high quality MeOH (HPLC grade) is required. The remaining solvents used
263 were dried and distilled before use.[39] Elemental analyses were performed at the Serveis de Científico-
264 Tècnics (Universitat de Barcelona). Mass spectrometry (ESI+) was performed at the Servei
265 d'Espectrometria de Masses (Universitat de Barcelona). The infrared spectra in the range $\tilde{\nu} = 4000\text{--}400$
266 cm^{-1} were obtained with a Nicolet 400 FTIR instrument with samples as KBr pellets, and far-IR spectra
267 were recorded with a Bomem-DA3 instrument by using polyethylene discs. Thin layer chromatography
268 (TLC) was performed with SiO₂ plates (Merck silica gel 60 F254). The UV/Vis spectra of solutions of
269 the compounds in CH₂Cl₂ were recorded at 298 K with a Cary 100 scan Varian UV spectrometer. The
270 routine ¹H NMR spectra were recorded with a Mercury 400 MHz instrument at the Indian Institute of
271 Chemical Biology of Kolkata and at the Serveis Científico-Tècnics (Universitat de Barcelona). The
272 high-resolution ¹H NMR spectra of the compounds dissolved in CDCl₃ (99.9%) containing SiMe₄ as an
273 internal reference were obtained with a Varian VRX-500 instrument or a Bruker Avance DMX 500
274 MHz instrument at 298 K. The ³¹P{¹H} (of 4) and ¹⁹⁵Pt{¹H} NMR spectra (of CDCl₃ solutions of 5
275 and 6) were recorded with a Varian 300 MHz instrument with P(OMe)₃ [δ (³¹P) = 140.17 ppm] and
276 H₂[PtCl₆] [δ (¹⁹⁵Pt) = 0.0 ppm], respectively, as references. The coupling constants (J) are given in Hz,
277 and chemical shifts (δ) are given in ppm.

278 **1-[MeO(CH₂)₂]-3,5-Ph₂-4-(CH₂Fc)-(C₃N₂) (1):** To a solution containing 3,5-Ph₂-4-(CH₂Fc)-
279 (C₃H_N₂) (IIa, 1.0 g, 2.39 $\times 10^{-3}$ mol)[17a] and toluene (30 mL), benzyltriethylammonium chloride
280 (BTAC; 136 mg, 6.0 $\times 10^{-4}$ mol) and an aqueous NaOH (40%) solution (7 mL) were added. Then, a
281 threefold excess of ClCH₂CH₂OMe (0.66 mL, 7.2 $\times 10^{-3}$ mol) was added dropwise to the mixture with
282 stirring. Once this process had finished, the resulting mixture was kept at 370 K for 24 h. After this
283 period, H₂O (50 mL) was added, and then the mixture was extracted with toluene (2 \times 25 mL). The
284 organic layers were combined, dried with Na₂SO₄, and then filtered. The resulting filtrate was
285 concentrated to dryness with a rotary evaporator. The residue was then dissolved in the minimum
286 amount of CH₂Cl₂ (5 mL) and passed through a short SiO₂ column (5.0 cm \times 2.0 cm). Elution with
287 CH₂Cl₂ produced a deep yellow band, which was collected and concentrated to dryness with a rotary
288 evaporator to give 1. The solid formed was then dried in vacuo for 2 d (yield: 911 mg, 80%).

289 **trans-[Pd{ κ -N-(1-{MeO(CH₂)₂}-3,5-Ph₂-4-{CH₂Fc}-{C₃N₂})}2Cl₂] (2):** This product can be
290 obtained with Na₂[PdCl₄] or cis-[PdCl₂(dmsO)₂] (methods a and b, respectively).

291 **Method a:** Ligand 1 (146 mg, 3.1 $\times 10^{-4}$ mol) was introduced to an Erlenmeyer flask, and then a
292 solution containing Na₂[PdCl₄] (45 mg, 1.5 $\times 10^{-4}$ mol) and MeOH (5 mL) was added. The resulting
293 mixture was protected from the light with aluminium foil and stirred at 298 K for 1 h. The yellow solid
294 formed was collected, washed with methanol (2 \times 2 mL portions), air-dried, and then dried in vacuo for 3
295 d (yield: 121 g, 70 %).

296 **Method b:** [PdCl₂(dmsO)₂] (50 mg, 1.5 $\times 10^{-4}$ mol) was suspended in methanol (30 mL), and the
297 suspension was heated under reflux until the solid dissolved completely. Then, the hot solution was
298 filtered, and the filtrate was poured into an Erlenmeyer flask containing ligand 1 (143 mg, 3.0 $\times 10^{-4}$
299 mol). The container was protected from the light with aluminium foil, and the reaction mixture was
300 heated under reflux for 2 h. The solid formed was collected, washed (as in method a), air-dried, and then
301 dried in vacuo for 2 d (yield: 137 mg, 80 %).

302 **[Pd{κ²-C,N-(1-{MeO(CH₂)₂}-3-{C₆H₄}-4-{CH₂Fc}-5-Ph-{C₃N₂})-(κ-N-1-{MeO(CH₂)₂}-3,5-**
303 **Ph₂-4-{CH₂Fc}-{C₃N₂})(OAc)] (3):** A mixture of 1 (238 mg, 5.0 × 10⁻³ mol), Pd(OAc)₂ (113 mg,
304 5.0 × 10⁻³ mol), and toluene (20 mL) was protected from the light with aluminium foil and heated under
305 reflux for 24 h. After this period, the hot mixture was carefully filtered through a Celite pad, and the
306 filtrate was cooled and kept aside. The Celite was then washed with small portions of CHCl₃ until
307 colorless mother liquors were obtained. These washings were combined with the filtrate and
308 concentrated to dryness with a rotary evaporator. The residue was then treated with the minimum
309 amount of CHCl₃ (ca. 5 mL) and passed through a SiO₂ chromatographic column (120 mm × 18 mm).
310 Elution with CHCl₃ produced a wide yellow band that gave small amounts of 1 (ca. 15 mg) after
311 concentration. Once this band was collected, a CHCl₃/MeOH mixture (100:1) produced the release of a
312 brownish band, which gave 3 after concentration by rotary evaporation. The solid formed was first air-
313 dried and dried in vacuo for 3 d (yield: 208 mg, 74%).

314 **[Pd{κ²-C,N-(1-{MeO(CH₂)₂}-3-{C₆H₄}-4-{CH₂Fc}-5-Ph-{C₃N₂})}Cl(PPh₃)] (4):** Compound 3
315 (115 mg, 1.0 × 10⁻⁴ mol) was dissolved in acetone (5 mL). Then, an excess of LiCl (6.5 mg, 1.5 × 10⁻⁴
316 mol) was added. The reaction mixture was protected from the light, stirred at 298 K for 1 h, and then
317 filtered. The filtrate was concentrated to dryness with a rotary evaporator, the residue was stored in a
318 SiO₂ desiccator overnight. The residue was then dissolved in the minimum amount of CH₂Cl₂ (ca. 15
319 mL) and treated with PPh₃ (27 mg, 1.0 × 10⁻⁴ mol); the mixture was stirred at 298 K for 1 h and then
320 filtered. The deep yellow solution was concentrated to ca. 5 mL with a rotary evaporator. After cooling
321 to room temperature, the solution was purified by SiO₂ column chromatography (3.0 × 1.2 cm²). Elution
322 with CH₂Cl₂ produced a pale yellow band, which gave the free ligand 1 (41 mg) after concentration to
323 dryness. Once this band was collected, a CH₂Cl₂/MeOH mixture (100:0.5) was used as the eluent. This
324 produced an additional band, which was collected and concentrated with a rotary evaporator to give 4 as
325 a brownish solid. This product was collected, air-dried, and finally dried in vacuo for 2 d (yield: 79 mg,
326 90 %). **trans-[Pt{κ-N-(1-{MeO(CH₂)₂}-3,5-Ph₂-4-{CH₂Fc}-{C₃N₂})}-Cl₂(dmsO)] (5):** cis-
327 **[PtCl₂(dmsO)₂] (225 mg, 5.3 × 10⁻⁴ mol)** was treated with methanol (20 mL). The resulting suspension
328 was protected from the light with aluminium foil, and the suspension was heated under reflux until the
329 solid dissolved completely. Then, the hot solution was carefully filtered, and the filtrate was poured into
330 an Erlenmeyer flask containing ligand 1 (269 mg, 5.3 × 10⁻⁴ mol). The resulting mixture was heated
331 under reflux for 1 h. After this period, the bright yellow solution was concentrated with a rotary
332 evaporator until a solid was obtained. The flask was cooled to ca. 298 K, and the solid that formed was
333 collected by filtration and dried in vacuo for 2 d (yield: 0.233 mg, 76%).

334 **cis-[Pt{κ-N-(1{MeO(CH₂)₂}-3,5-Ph₂-4-{CH₂Fc}-{C₃N₂})}-Cl₂(dmsO)] (6)·CH₂Cl₂·MeOH:**
335 Ligand 1 (254 mg, 5.3 × 10⁻⁴ mol) and cis-[PtCl₂(dmsO)₂] (225 mg, 5.3 × 10⁻⁴ mol) were dissolved in
336 toluene (20 mL). Then, a solution containing an equimolar amount of NaOAc (87 mg, 1.06 × 10⁻³)
337 dissolved in MeOH (5 mL) was added dropwise with stirring at 298 K. The reaction mixture was heated
338 under reflux for 24 h. After this period, the deep orange solution that formed was filtered, and the filtrate
339 was concentrated to dryness with a rotary evaporator and kept in a desiccator overnight. The residue was
340 then dissolved in the minimum amount of CH₂Cl₂. The undissolved products were removed by
341 filtration, and the filtrate was passed through a short SiO₂ column (4.0 cm × 1.0 cm). Elution with
342 CH₂Cl₂ produced a yellowish band, which gave the trans isomer 5 (67 mg) after concentration. Next, a
343 mixture of CH₂Cl₂/MeOH (100:1) was used, and the orange band was concentrated to dryness by rotary
344 evaporation. The solid formed, 6, was collected, air-dried for 24 h, and then dried in vacuo for 2 d (259
345 mg). Crystals of 6·CH₂Cl₂·MeOH were obtained at 298 K by the slow evaporation of a saturated
346 solution of 6 in CH₂Cl₂ layered with an identical volume of MeOH.

347 **Crystallography:** Prismlike crystals of 2 and 6·CH₂Cl₂·MeOH (sizes in Table 3) were used for the X-
348 ray crystallographic analysis. The X-ray intensity data were measured with a D8 Venture system
349 equipped with a multilayer monochromator and a Mo high-brilliance Microfocus Source (λ = 0.71073
350 Å). The frames were integrated with the Bruker SAINT software package by using a narrow-frame

351 algorithm. The final cell constants (Table 3) are based upon the refinement of the XYZ centroids of
352 3561 reflections above $2\sigma(I)$ with $5.11 \square 2\theta \square 50.26^\circ$. The data were corrected for absorption effects by
353 the multiscan method (SADABS). The ratio of minimum to maximum apparent transmission was 0.779.

354 For 2, the integration of the data with a monoclinic unit cell yielded a total of 10506 reflections to a
355 maximum θ angle of 25.13° (0.84 \AA resolution), of which 4519 were independent (average redundancy
356 2.325, completeness: 98.8%, $R_{int} = 4.42\%$) and 3146 (69.62%) were greater than $2\sigma(F_2)$. For
357 $6 \cdot \text{CH}_2\text{Cl}_2 \cdot \text{MeOH}$, the integration of the data with a monoclinic unit cell yielded a total of 28067
358 reflections to a maximum θ angle of 25.11° (0.84 \AA resolution), of which 6261 were independent
359 (average redundancy 4.483, completeness: 99.4%, $R_{int} = 8.20\%$, $R_{sig} = 4.65\%$) and 5497 (87.80%)
360 were greater than $2\sigma(F_2)$.

361 These structures were solved and refined with the Bruker SHELXTL software package[40] in the space
362 groups P21/c (for 2) and C2/c (for $6 \cdot \text{CH}_2\text{Cl}_2 \cdot \text{MeOH}$). The final anisotropic full-matrix least-squares
363 refinement on F_2 with 302 (for 2) or 413 (for $6 \cdot \text{CH}_2\text{Cl}_2 \cdot \text{MeOH}$) variables converged at $R_1 = 6.58$ (for
364 the observed data and $wR_2 = 17.62\%$ for all data) and 3.94% (for the observed data and $wR_2 = 10.92\%$
365 for all data), respectively. The goodness-of-fit values were 1.044 (for 2) and 1.028 (for
366 $6 \cdot \text{CH}_2\text{Cl}_2 \cdot \text{MeOH}$).

367 For 2, the largest peak in the final difference electron density synthesis was 2.237 e/\AA^3 and the largest
368 hole was -1.473 e/\AA^3 with a root mean square (RMS) deviation of 0.128 e/\AA^3 . On the basis of the final
369 model, the calculated density was 1.465 g/cm^3 , and $F(000)$ was 1160 e. For $6 \cdot \text{CH}_2\text{Cl}_2 \cdot 2\text{MeOH}$, the
370 largest peak in the final difference electron density synthesis was 2.521 e/\AA^3 , and the largest hole was $-$
371 2.829 e/\AA^3 with an RMS deviation of 0.182 e/\AA^3 . On the basis of the final model, the calculated density
372 was 1.792 g/cm^3 , and $F(000)$ was 3760 e $^-$.

373 CCDC-1014331 (for 2) and -1014332 (for $6 \cdot \text{CH}_2\text{Cl}_2 \cdot \text{MeOH}$) contain the supplementary
374 crystallographic data for this paper. These data can be obtained free of charge from The Cambridge
375 Crystallographic Data Centre via www.ccdc.cam.ac.uk/data_request/cif. **Cell Cultures:** Breast cancer
376 (MCF7 and MDA-MB231) cells (from European Collection of Cell Cultures, ECACC) and colon
377 adenocarcinoma (HCT116) cells (from the American Type Culture Collection) were used in all of the
378 experiments. The cells were grown as monolayer cultures in minimum essential medium (DMEM with
379 l-glutamine, without glucose and without sodium pyruvate) in the presence of 10% heat-inactivated fetal
380 calf serum, 10 mm d-glucose, and 0.1% streptomycin/penicillin under standard culture conditions.

381 **Cell Viability Assays:** For these studies, the compounds were dissolved in 100% DMSO at 50 mm as
382 stock solutions; then, serial dilutions were performed with DMSO (1:1; in this way, the DMSO
383 concentrations in the cell media were always the same); finally, 1:500 dilutions of the serially diluted
384 solutions of the compounds on the cell media were performed. The assays were performed as described
385 by Givens et al.[41] In brief, MDA-MB231 and MCF7 cells were plated at 5000 and 10000 cells/well,
386 respectively, in media (100 μL) in tissue culture 96-well plates (Cultek). After 24 h, the media was
387 replaced by 100 μL /well of serial dilutions of the drugs. Each point concentration was run in triplicate.
388 Reagent blanks, containing media plus colorimetric reagent without cells were run on each plate. The
389 blank values were subtracted from the test values and were routinely 5–10% of the uninhibited control
390 values. The plates were incubated for 72 h. The hexosaminidase activities were measured according to
391 the following protocol: the media containing the cells were removed, and the cells were washed once
392 with phosphate-buffered saline (PBS), and substrate solution [60 μL ; pnitrophenyl N-acetyl- β -d-
393 glucosamide 7.5 mm (Sigma N-9376), sodium citrate 0.1 m, pH 5.0, 0.25% Triton X-100] was added to
394 each well and incubated at 37°C for 1–2 h; after this incubation time, a bright yellow color appeared;
395 then, the plates were developed by the addition of developer solution [90 μL ; Glycine 50 mm, pH 10.4;
396 ethylenediaminetetraacetic acid (EDTA) 5 mm], and the absorbance was recorded at 410 nm.

397

398 **Supporting Information** (see footnote on the first page of this article): Characterization data (elemental
399 analyses, MS, IR, UV/Vis, and NMR spectroscopy) for 1–6 and crystal structures of 2 and
400 6·CH₂Cl₂·MeOH.

401

402

403 **ACKNOWLEDGEMENTS**

404

405 This work was supported by the Ministerio de Ciencia e Innovación (MICINN) (grant numbers
406 CTQ2009-11501 and TEC2011-29140-C03-02) and by the Government of India, Department of Science
407 and Technology (DST), New Delhi, Grant Fasttrack Scheme SR/FT/CS-049/2008. A. G. is grateful to
408 DST, New Delhi for providing a research fellowship.

409

410

- 411 [1] a) J. Elguero, Pyrazoles and Their Benzo Derivatives, in: *Comprehensive Heterocyclic*
412 *Chemistry*, vol. 5 (Eds.: A. R. Katritzky, C. W. Rees), Pergamon Press, Oxford, UK, 1984, p.
413 167–303, chapter 4.04; b) J. Elguero, Pyrazoles, in: *Comprehensive Heterocyclic Chemistry II*,
414 vol. 3 (Eds.: A. R. Katritzky, W. Rees, E. F. V. Scrivens), Pergamon Press, Oxford, UK, 1996, p.
415 1–75, chapter 3.01; c) J. J. Li, *Heterocyclic Chemistry in Drug Discovery*, John Wiley & Sons,
416 Hoboken, 2013, p. 198–229.
- 417 [2] a) F. K. Keter, I. Darkwa, *Biometals* 2012, 25, 9–21; b) H. Kumar, D. Saini, S. Jain, N. Jain,
418 *Eur. J. Med. Chem.* 2013, 70, 248–258; c) V. Kumar, K. Kaur, G. K. Gupta, A. K. Sharma, *Eur.*
419 *J. Med. Chem.* 2013, 69, 735–753; d) S. K. Tambe, N. S. Dighe, S. R. Pattan, M. S. Kedar, D. S.
420 Musmade, *Pharmacologyonline* 2010, 2, 5–16; e) J. Elguero, P. Goya, N. Jagerovic, A. M. S.
421 Silva, *Targets Heterocycl. Syst.* 2002, 6, 52–98; f) J. Elguero, A. M. S. Silva, A. C. Tome, *Mod.*
422 *Heterocycl. Chem.* 2011, 2, 635–725; g) A. Schmidt, A. Dreger, *Curr. Org. Chem.* 2011, 15,
423 1423–1463.
- 424 [3] For reviews on bioactive pyrazoles, see, for instance: a) L. Yet, *Prog. Heterocycl. Chem.* 2013,
425 25, 217–256; b) L. Yet, *Prog. Heterocycl. Chem.* 2012, 24, 243–279; c) L. Pizzuti, A. G.
426 Barschak, F. M. Stefanello, M. D. Farias, C. Lencina, M. Roesch-Ely, W. Cunico, S. Moura, C.
427 M. P. Pereira, *Curr. Org. Chem.* 2014, 18, 115–126; d) G. K. Gupta, A. Mittal, V. Kumar,
428 *Lett. Org. Chem.* 2014, 11, 273–286.
- 429 [4] a) M. Amir, K. Somakala, S. Ali, *Mini-Rev. Med. Chem.* 2013, 13, 2082–2096; b) J. Reis, I.
430 Encarnacao, A. Gaspar, A. Morales, N. Milhazes, F. Borges, *Curr. Top. Med. Chem.* 2012, 12,
431 2116–2130; c) D. Secci, S. Carradori, A. Bolasco, B. Bizzarri, M. D’Ascenzio, E. Maccioni,
432 *Curr. Top. Med. Chem.* 2012, 12, 2240–2257; d) A. A. Bekhit, A. Hymete, A.-E.-D. A. Bekhit,
433 A. Damte, H. Y. Aboul-Enein, *Mini-Rev. Med. Chem.* 2010, 10, 1014–1033; e) I.
434 Vujasinovic’, A. Paravic’-Radic’evic’, K. Mlinaric ’-Majerski, K. Brajs’a, B. Bertos’a, *Bioorg.*
435 *Med. Chem.* 2012, 20, 2101–2110.
- 436 [5] a) R. Aggarwal, V. Kumar, G. K. Gupta, V. Kumar, K. Vinod, *Med. Chem. Res.* 2013, 22,
437 3566–3573; b) P. Horrocks, M. R. Pickard, H. H. Parekh, S. P. Patel, R. B. Pathak, *Org. Biomol.*
438 *Chem.* 2013, 11, 4891–4898.
- 439 [6] a) *Comprehensive Coordination Chemistry II* (Eds.: J. A. McCleverty, T. J. Meyer), Elsevier,
440 Amsterdam, 2003; b) *Comprehensive Organometallic Chemistry III* (Eds.: H. Crabtree, D. M. P.
441 Mingos), 3rd ed., Elsevier, Amsterdam, 2007.
- 442 [7] For recent reviews on pyrazole derivatives, see: a) J. Garcia-Anton, R. Bofill, L. Escriche, A.
443 Llobet, X. Sala, *Eur. J. Inorg. Chem.* 2012, 4775–4789; b) S. Kuwata, T. Ikariya, *Chem. Eur. J.*
444 2011, 17, 3542–3556; c) M. Viciano-Chumillas, S. Tanase, L. Jos de Jongh, J. Reedijk, *Eur. J.*
445 *Inorg. Chem.* 2010, 3403–3418; d) S. O. Ojwach, J. Darkwa, *Inorg. Chim. Acta* 2010, 363,
446 1947–1964; e) J. Pérez, L. Riera, *Eur. J. Inorg. Chem.* 2009, 4913–4925; f) J. Klingele, S.
447 Dechert, F. Meyer, *Coord. Chem. Rev.* 2009, 253, 2698–2741.

- 448 [8] For recent examples of PdII and PtII complexes containing pyrazole ligands, see: a) C. V. Barra,
449 F. V. Rocha, A. V. G. Netto, R. C. G. Frem, A. E. Mauro, I. Z. Carlos, S. R. Ananias, M. B.
450 Quilles, *J. Therm. Anal. Calorim.* 2011, 106, 489–494; b) C. V. Barra, F. V. Rocha, A. V. G.
451 Netto, B. Shimura, R. C. G. Frem, A. E. Mauro, I. Z. Carlos, S. R. Ananias, M. B. Quilles, *J.*
452 *Therm. Anal. Calorim.* 2011, 106, 483–488; c) E. Budzisz, M. Miernicka, I.-P. Lorenz, P.
453 Mayer, E. Balcerczak, U. Krajewska, M. Rozalski, *Eur. J. Med. Chem.* 2010, 45, 2613–2621; d)
454 A. S. Abu-Surrah, K. A. Abu-Safieh, I. M. Ahmad, M. Y. Addalla, M. T. Ayoub, A. K.
455 Qaroush, A. M. Abu-Mahtheieh, *Eur. J. Med. Chem.* 2010, 45, 471–475; e) C. Francisco, S.
456 Gama, F. Mendes, F. Marques, I. Cordeiro dos Santos, A. Paulo, I. Santos, J. Coimbra, E.
457 Gabano, M. Ravera, *Dalton Trans.* 2011, 40, 5781–5792.
- 458 [9] a) J. U. Chukwu, C. López, A. González, M. Font-Bardía, M. T. Calvet, R. Messeguer, C.
459 Calvis, *J. Organomet. Chem.* 2014, 766, 13–21; b) J. Quirante, D. Ruiz, A. González, C. López,
460 M. Cascante, R. Cortés, R. Messeguer, C. Calvis, L. Baldomà, A. Pascual, Y. Guérardel, B.
461 Pradines, M. Font-Bardía, T. Calvet, C. Biot, *J. Inorg. Biochem.* 2011, 105, 1720–1728; c) J.
462 Chakraborty, M. K. Saha, P. Benerjee, *Inorg. Chem. Commun.* 2007, 10, 671–676; d) R. Y.
463 Mawo, D. M. Johnson, J. L. Wood, I. P. Smoliakova, *J. Organomet. Chem.* 2008, 693, 33–45.
- 464 [10] For reviews on bioorganometallic chemistry, see: a) R. S. Herrick, C. J. Ziegler, T. C. Leeper, J.
465 *Organomet. Chem.* 2014, 751, 90–110; b) T. Dallagi, M. Siadi, A. Vessieres, M. Huche, G.
466 Jaouen, S. Top, *J. Organomet. Chem.* 2013, 734, 69–77; c) A. Monney, M. Albrecht, *Coord.*
467 *Chem. Rev.* 2013, 257, 2420–2433; d) A. L. Noffke, A. Habtemariam, A. M. Pizarro, P. J.
468 Sadler, *Chem. Commun.* 2012, 48, 5219–5246; e) C. Biot, D. Dive, *Top. Organomet. Chem.*
469 2010, 32, 155–193; f) N. Chavain, C. Biot, *Curr. Med. Chem.* 2010, 17, 2729; g) R. H. Fish,
470 *Aust. J. Chem.* 2010, 63, 1505–1513; h) S. El Kazzouli, N. El Brahmi, S. Mignani, M.
471 Bousmina, M. Zablocka, J.-P. Majoral, *Curr. Med. Chem.* 2012, 19, 4995–5010; i) E. A. Hillard,
472 G. Jaouen, *Organometallics* 2011, 30, 20–27; j) G. Gasser, I. Ott, N. Metzler-Nolte, *J. Med.*
473 *Chem.* 2011, 54, 3–25.
- 474 [11] See, for instance: a) F. Dubar, C. Slomianny, J. Khalife, D. Dive, H. Kalamou, Y. Guérardel, P.
475 Grellier, C. Biot, *Angew. Chem. Int. Ed.* 2013, 52, 7690–7693; b) R. Arancibia, C. Biot, G.
476 Delaney, P. Roussel, A. Pascual, B. Pradines, A. H. Klahn, *J. Organomet. Chem.* 2013, 723,
477 143–148; c) M. A. L. Blackie, *Mini-Rev. Med. Chem.* 2013, 13, 597–606; d) M. Patra, K.
478 Ingram, A. Leonidova, V. Pierroz, S. Ferrari, M. N. Robertson, M. H. Todd, J. Keiser, G.
479 Gasser, *J. Med. Chem.* 2013, 56, 9192–9198.
- 480 [12] P. Stepnicka (Ed.), *Ferrocenes: Ligands, Materials and Biomolecules*, Wiley, Weinheim,
481 Germany, 2008.
- 482 [13] a) S. Li, Z. Wang, Y. Wei, C. Wu, S. Gao, H. Jiang, X. Zhao, H. Yang, X. Wang, *Biomaterials*
483 2013, 34, 902–911; b) N. Nguyen, A. Vessièrès, E. A. Hillard, S. Top, P. Pigeon, G. Jaouen,
484 *Chimia* 2007, 61, 716–724.

- 485 [14] For relevant contributions in this field, see: a) R. Arancibia, A. H. Klahn, G. E. Buono-Core, D.
486 Contreras, G. Barriga, C. Olea-Azar, M. Lapier, J. D. Maya, A. Ibañez, M. T. Garland, J.
487 Organomet. Chem. 2013, 743, 49–54; b) A. Gul, Z. Akhter, M. Siddiq, S. Sarfraz, B. Mirza,
488 Macromolecules 2013, 46, 2800–2807; c) A. I. Mufula, B. A. Aderibigbe, E. W. Neuse, H. E.
489 Mukaya, J. Inorg. Organomet. Polym. Mater. 2012, 22, 423–428; d) S. Knauer, B. Biersack, M.
490 Zoldakova, K. Effenberger, W. Milius, R. Schobert, *Anti-Cancer Drugs* 2009, 20, 676–681.
- 491 [15] M. F. R. Fouda, M. M. Abd-Elzaher, R. A. Abdelsamai, A. A. Labib, *Appl. Organomet. Chem.*
492 2007, 21, 613–635.
- 493 [16] a) X. F. Huang, L. Z. Wang, L. Tang, Y.-X. Lu, F. Wang, G.-Q. Song, B.-F. Ruan, J.
494 *Organomet. Chem.* 2014, 749, 157–162; b) S. L. Shen, J. Zhu, M. Li, B.-X. Zhao, J.-X. Miao,
495 *Eur. J. Med. Chem.* 2012, 54, 287–294; c) W. C. Duivenvoorden, Y. Liu, G. Schatte, H. B.
496 Kraatz, *Inorg. Chim. Acta* 2005, 358, 3183–3185; d) M. Auzias, J. Gueniat, B. Therrien, G.
497 Süss-Fink, A. K. Renfrew, P. J. Dyson, *J. Organomet. Chem.* 2009, 694, 855–861; e) M. Zora,
498 A. N. Pinar, M. Odabasoglu, O. Buyukgungor, G. Turgut, *J. Organomet. Chem.* 2008, 693, 145–
499 154; f) M. Zora, M. Gormen, *J. Organomet. Chem.* 2007, 692, 5026–5032; g) L. Gaina, A.
500 Csampai, G. Turos, T. Lovasz, V. Zsoldos-Mady, I. A. Silberg, P. Sohar, *Org. Biomol. Chem.*
501 2006, 4, 4375–4386; h) W.-C. Shen, Y.-J. Wang, K.-L. Cheng, G.-H. Lee, C. K. Lai,
502 *Tetrahedron* 2006, 62, 8035–8044; i) A. N. Rodionov, A. A. Simenel, A. A. Korlyukov, V. V.
503 Kachala, S. M. Peregudova, K. Y. Zherebker, E. Y. Osipova, *J. Organomet. Chem.* 2011, 696,
504 2108–2115; j) A. H. Ilkhechi, M. Bolte, H.-W. Lerner, M. Wagner, *J. Organomet. Chem.* 2005,
505 690, 1971–1977; k) E. I. Klimova, E. A. López, T. Klimova, C. A. Toledano, R. A. Toscano, M.
506 M. Garcia, *J. Heterocycl. Chem.* 2005, 42, 265–271; l) A. Magistrato, T. K. Woo, A. Togni, U.
507 Rothlisberger, *Organometallics* 2004, 23, 3218–3227.
- 508 [17] For examples of PdII and PtII complexes containing hybrid ferrocene–pyrazole ligands, see: a)
509 C. López, A. González, R. Bosque, P. K. Basu, M. Font-Bardía, T. Calvet, *RSC Adv.* 2012, 2,
510 1986–2002; b) P. K. Basu, A. González, C. López, M. Font-Bardía, T. Calvet, *J. Organomet.*
511 *Chem.* 2009, 694, 3633–3642.
- 512 [18] A. González, C. López, X. Solans, M. Font-Bardía, E. Molins, *J. Organomet. Chem.* 2008, 693,
513 2119–2131.
- 514 [19] G. Pfeiffer, H. Bauer, *Liebigs Ann. Chem.* 1980, 564–576.
- 515 [20] F. H. Allen, *Acta Crystallogr., Sect. B* 2002, 58, 380–388.
- 516 [21] S. Muñoz, J. Pons, J. Ros, M. Font-Bardía, C. A. Kilner, M. A. Halcrow, *Inorg. Chim. Acta*
517 2011, 373, 211–218.
- 518 [22] For PdII complexes with agostic interactions, see, for instance: a) H. R. Thomas, R. J. Deeth, G.
519 J. Clarkson, J. P. Rourke, *Organometallics* 2011, 30, 5641–5648; b) M. P. Mitoraj, A. Michalak,
520 T. Ziegler, *Organometallics* 2009, 28, 3727–3733; c) H. V. Huynh, Y. Han, J. H. H. Ho, G. K.

- 521 Tan, *Organometallics* 2006, 25, 3267–3274; d) L. H. Shultz, M. Brookhart, *Organometallics*
522 2001, 20, 3975–3982.
- 523 [23] See, for instance: S.-I. Morita, A. Fujii, N. Mikami, S. Tsuzuki, *J. Phys. Chem. A* 2006, 110,
524 10583–10590.
- 525 [24] a) I. Omae, *Cyclometallation Reactions: Five-Membered Ring Products as Universal Reagents*,
526 Springer, New York, 2014; b) J. Dupont, M. Pfeffer (Eds.), *Palladacycles: Synthesis*
527 *Characterization and Applications*, Wiley-VCH, Weinheim, Germany, 2008.
- 528 [25] For recent reviews on this topic, see: a) I. Omae, *Coord. Chem. Rev.* 2014, 280, 84–95; b) I.
529 Omae, *Curr. Org. Chem.* 2014, 18, 2776–2794.
- 530 [26] For recent contributions on palladacycles with antitumoral activity, see: a) S. Aliwaini, A. J.
531 Swarts, A. Blankenberg, S. Mapolie, S. Prince, *Biochem. Pharmacol.* 2013, 1650–1663; b) J.
532 Albert, S. García, J. Granell, A. Llorca, M. V. Lovelle, V. Moreno, A. Presa, L. Rodríguez, J.
533 Quirante, C. Calvis, R. Messeguer, J. Badía, L. Baldomà, *J. Organomet. Chem.* 2013, 724, 289–
534 296; c) K. Karami, M. H. Kharat, H. Sadeghi-Aliabadi, J. Lipkowski, M. Mirian, *Polyhedron*
535 2012, 50, 187–192; d) M. Carreira, R. Calvo-Sanjuan, M. Sanau, I. Marzo, M. Contel,
536 *Organometallics* 2012, 31, 5772–5781; e) J. Spencer, R. P. Rathnam, M. Motukuri, A. K. Kotha,
537 S. C. W. Richardson, A. Hazrati, J. A. Hartley, L. Male, M. B. Hursthouse, *Dalton Trans.* 2009,
538 4299–4303; f) F. A. Serrano, A. L. Matsuo, P. T. Monteforte, A. Bechara, S. S. Smaili, D. P.
539 Santana, T. Rodrigues, F. V. Pereira, L. S. Silva, J. Machado, E. L. Santos, J. B. Pesquero, R. M.
540 Martins, L. R. Travassos, A. C. F. Caires, E. G. Rodrigues, *BMC Cancer* 2011, 11, 296–312.
- 541 [27] For recent advances on platinacycles with antitumoral activity, see: a) D. Talancón, C. López,
542 M. Font-Bardía, T. Calvet, J. Quirante, C. Calvis, R. Messeguer, R. Cortes, M. Cascante, L.
543 Baldomà, J. Badía, *J. Inorg. Biochem.* 2013, 118, 1–12; b) R. Cortés, M. Crespo, L. Davin, R.
544 Martín, J. Quirante, D. Ruiz, R. Messeguer, C. Calvis, L. Baldomà, J. Badía, M. Font-Bardía, T.
545 Calvet, M. Cascante, *Eur. J. Med. Chem.* 2012, 54, 557–566; c) J. Albert, R. Bosque, M.
546 Crespo, J. Granell, C. López, R. Cortés, A. González, J. Quirante, C. Calvis, R. Messeguer, L.
547 Baldomà, J. Badía, M. Cascante, *Bioorg. Med. Chem.* 2013, 21, 4210–4217; d) R. Cortés, M.
548 Tarrado-Castellarnau, D. Talancón, C. López, W. Link, D. Ruiz, J. J. Centelles, J. Quirante, M.
549 Cascante, *Metallomics* 2014, 6, 622–633; e) D. A. K. Veezu, Q. Lu, Y.-H. Chen, S. Huo, J.
550 *Inorg. Biochem.* 2014, 134, 49–56.
- 551 [28] K. Nakamoto, *Infrared and Raman Spectra of Inorganic and Coordination Compounds*, 5th ed.,
552 Wiley, New York, 1997.
- 553 [29] J. Albert, R. Bosque, M. Cadena, L. D’Andrea, J. Granell, A. González, J. Quirante, C. Calvis,
554 R. Messeguer, J. Badía, L. Baldomà, T. Calvet, M. Font-Bardía, *Organometallics* 2014, 33,
555 2862–2873.
- 556 [30] X. Riera, A. Caubet, C. López, V. Moreno, X. Solans, M. Font-Bardía, *Organometallics* 2000,
557 19, 1384–1390.

- 558 [31] S. Pérez, C. López, A. Caubet, X. Solans, M. Font-Bardía, M. Gich, E. Molins, *J. Organomet.*
559 *Chem.* 2007, 692, 2402–2414.
- 560 [32] J. Vicente, J. A. Abad, A. D. Frankland, M. C. Ramírez de Arellano, *Chem. Eur. J.* 1999, 5,
561 3066–3075.
- 562 [33] J. H. Price, A. N. Williamson, R. F. Schramm, B. B. Wayland, *Inorg. Chem.* 1972, 11, 1280–
563 1284.
- 564 [34] For recent reviews, see: a) N. Muhnammad, Z. Guo, *Curr. Opin. Chem. Biol.* 2014, 19, 144–
565 153; b) D. Wyrzykowska, L. Chimurzynski, *Curr. Pharmaceut. Anal.* 2014, 10, 2–9.
- 566 [35] For recent studies, see: a) M. Sirisi, V. Gardin, T. Saltarella, F. P. Intini, C. Pacifico, C.
567 Marzano, G. Natile, *J. Biol. Inorg. Chem.* 2014, 19, 1081–1079; b) C. Pérez, C. V. Diaz-García,
568 A. Agudo-López, V. del Solar, S. Cabero, M. Agullo-Ostuno, C. Navarro-Ranninger, J. Alemán,
569 J. A. López-Martin, *Eur. J. Med. Chem.* 2014, 76, 360–368.
- 570 [36] C. López, A. Caubet, S. Pérez, X. Solans, M. Font-Bardía, E. Molins, *Eur. J. Inorg. Chem.* 2006,
571 3974–3984.
- 572 [37] B. M. Still, P. G. A. Kumar, J. R. Aldrich-Wright, W. S. Price, *Chem. Soc. Rev.* 2007, 36, 665–
573 686.
- 574 [38] Z. Szafran, R. M. Pike, M. M. Singh, *Microscale Inorganic Chemistry: A Comprehensive*
575 *Laboratory Experience*, John Wiley & Sons, New York 1991, p. 218.
- 576 [39] D. D. Perrin, W. L. F. Armarego, *Purification of Laboratory Chemicals*, 4th ed., Butterworth-
577 Heinemann, Oxford, UK, 1996.
- 578 [40] G. M. Sheldrick, *Acta Crystallogr., Sect. A* 2008, 64, 112–122.
- 579 [41] K. T. Givens, S. Kitada, A. K. Chen, J. Rothschilder, D. A. Lee, *Invest. Ophth. Vis. Sci.* 1990,
580 31, 1856–1862.
- 581 .

582 **Legends to figures**

583

584 **Figure 1.** Selected 3,5-disubstituted pyrazoles (I–V) described previously, the new ligand used in this
585 work (1), and the PdII complex trans-[Pd{ κ -N-(1-{MeO(CH₂)₂}-3,5-Ph₂-{C₃HN₂})}2Cl₂] (Va).

586

587 **Scheme 1.** i) Toluene, benzyltriethylammonium chloride (BTAC), NaOH (40 %), and MeO(CH₂)₂Cl at
588 370 K for 24 h.

589

590 **Scheme 2.** i) Na₂[PdCl₄] in MeOH (298 K, 1 h) or [PdCl₂(dmsO)₂] in MeOH, reflux, 1 h (molar ratios
591 1/PdII = 1 or 2, see text and Table 1, Entries 1 and 2); ii) Pd(OAc)₂, toluene, reflux, 24 h; iii) SiO₂
592 column chromatography; iv) LiCl (50% excess) in acetone at 298 K (1 h) followed by treatment with
593 PPh₃ (molar ratio 3/PPh₃ = 1:1) in CH₂Cl₂ at 298 K for 1 h; v) cis-[PtCl₂(dmsO)₂] in MeOH, reflux;
594 vi) cis-[PtCl₂(dmsO)₂] and NaOAc (molar ratio 1/PtII/OAc⁻ = 1:1:2), toluene/methanol (5:1), reflux, 24
595 h.

596

597 **Figure 2.** Molecular structure of 2. Hydrogen atoms have been omitted for clarity. Selected bond
598 lengths [Å] and angles [°]: Pd1–N1 2.007(4), Pd1–Cl1 2.3013(17), C22–O1 1.465(10), N2–C13,
599 1.354(8), N2–N1 1.364(7), N2–C20 1.460(8), O1–C21 1.390(9), N1–C24 1.336(8), C20–C21 1.495(11),
600 C13–C12 1.387(9), C13–C14 1.479(9), Fe–C (average value of Fc moiety) 2.037(9), C–C (average for
601 Fc) 1.41(4), N1–Pd1–Cl1 88.95(14).

602

603 **Figure 3** Molecular structure of the dimetallic molecules in the crystal structure of 6·CH₂Cl₂·MeOH.
604 Solvation molecules and hydrogen atoms have been omitted for clarity. Selected bond lengths [Å] and
605 angles [°]: Pt1–N1 2.0127(4), Pt1–S1 2.2037(13), Pt1–Cl1 2.2868(12), Pt1–Cl2 2.3184(13), S1–O1
606 1.466(4), S1–C30 1.766(6), S1–C31 1.778(6), O2–C28 1.409(6), O2–C29 1.429(6), N1–C13 1.338(6),
607 N1–N2 1.364(5), N2–C14 1.362(6), N2–C(27) 1.455(6), Fe–C (Fc unit) 2.044(6), C–C (average value
608 for the Fc moiety) 1.42(1), N1–Pt1–S1 91.89(12), S1–Pt1–Cl1 90.79(5), N1–Pt1–Cl2 87.34(12).

609

610 **Figure 4.** Comparative plot of the IC₅₀ values [μm] of 1, V, their closely related derivative IV, and
611 cisplatin against the MCF7 and MDA-MB231 breast cancer cell lines.

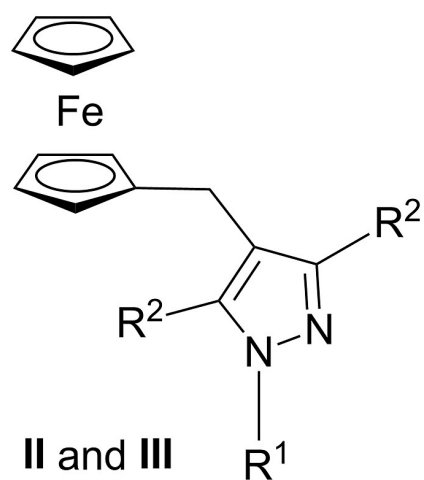
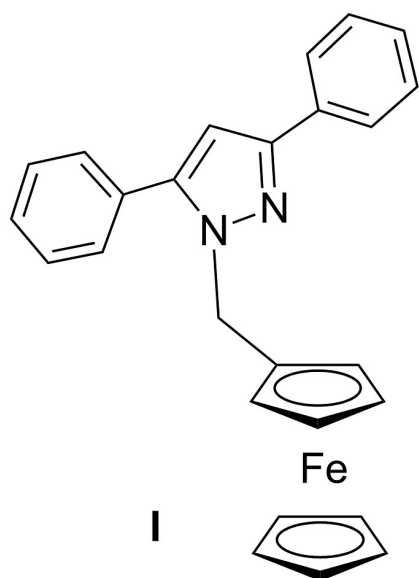
612

613 **Figure 5** Comparative plot of the IC₅₀ values [μm] of the free ligand 1, the PdII complexes 2–4, and the
614 trans and cis isomers of [Pt{ κ -N-(1-{MeO(CH₂)₂}-3,5-Ph₂-4-{CH₂Fc}-{C₃N₂})}Cl₂- (dmsO)] (5 and
615 6, respectively) against the MCF7 and MDAMB231 breast cancer cell lines and the cisplatin-resistant
616 colon cancer cell line (HCT-116). For comparison, the data obtained for cisplatin under identical
617 experimental conditions are also included.

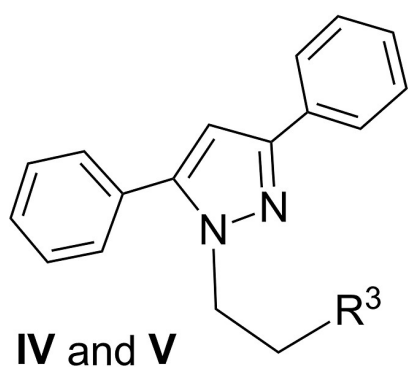
618

619
620
621

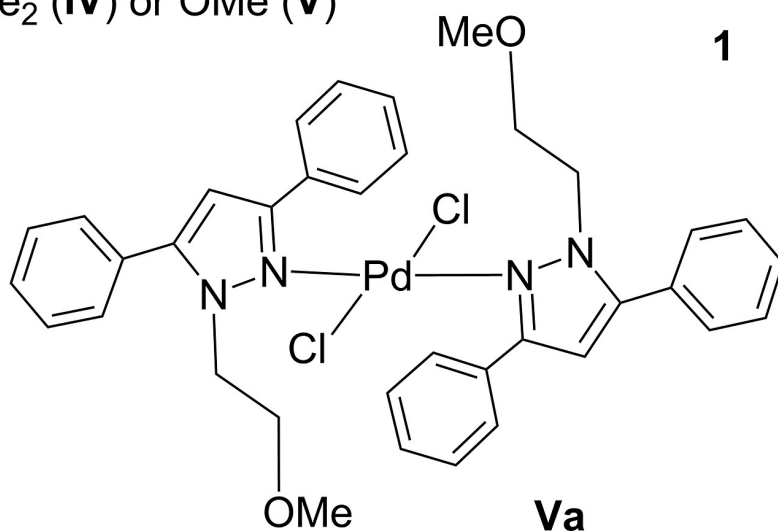
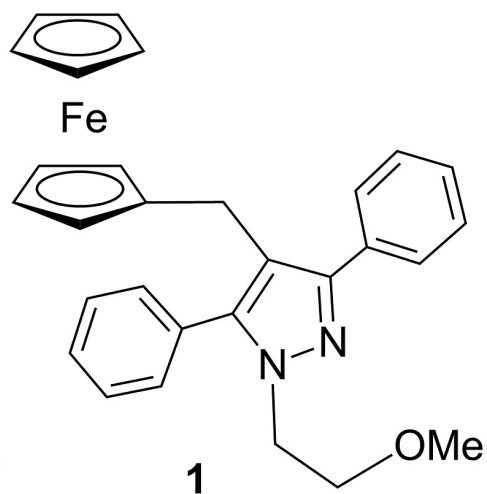
FIGURE 1.



II R¹ = H and R² = Ph (**IIa**) or Me (**IIb**)
III R¹ = Me and R² = Ph (**IIIa**) or Me (**IIIb**)



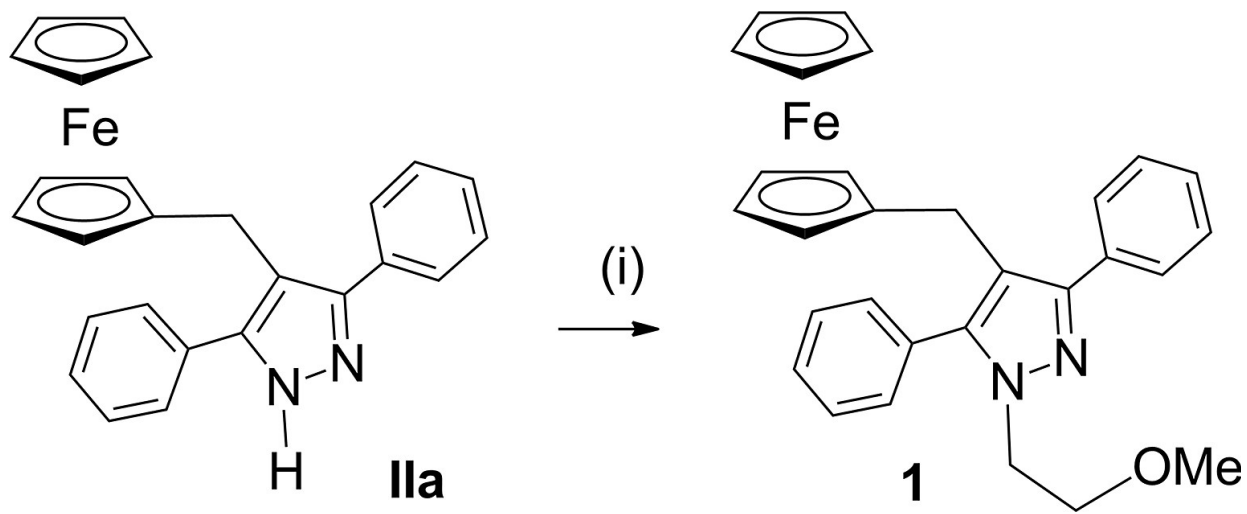
R³ = NMe₂ (**IV**) or OMe (**V**)



622
623

624
625
626

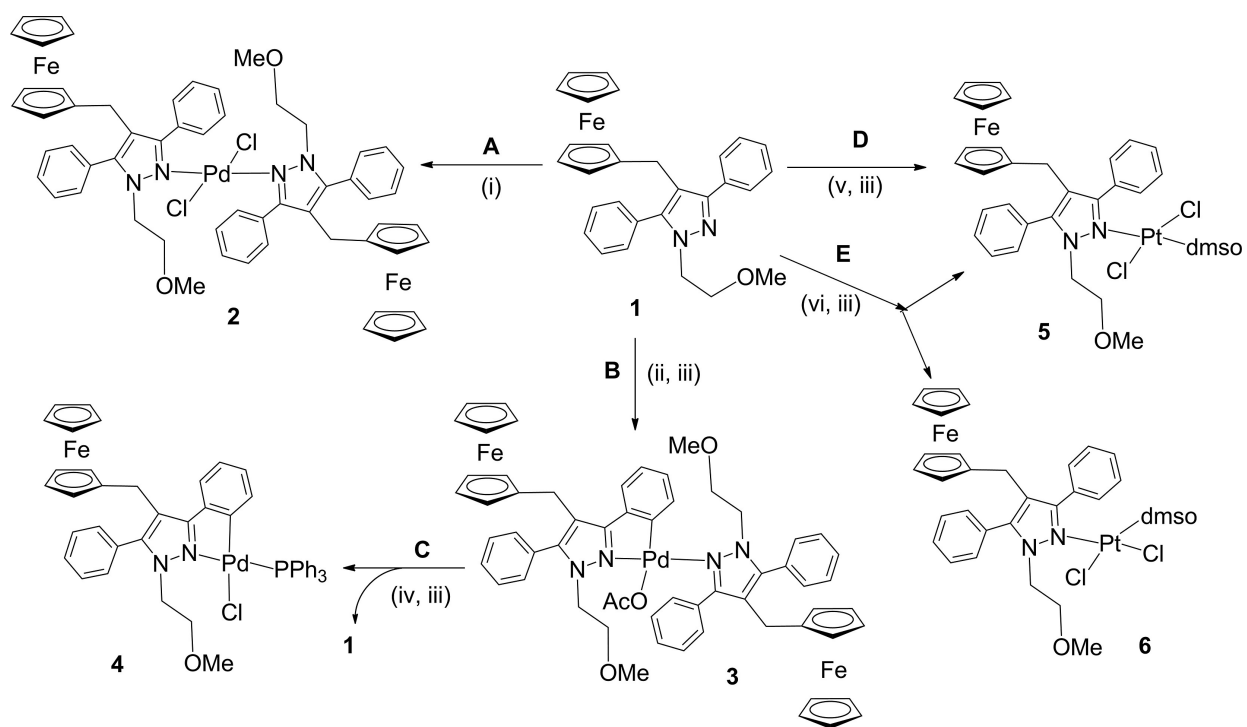
SCHEME 1.



627
628

629
630
631

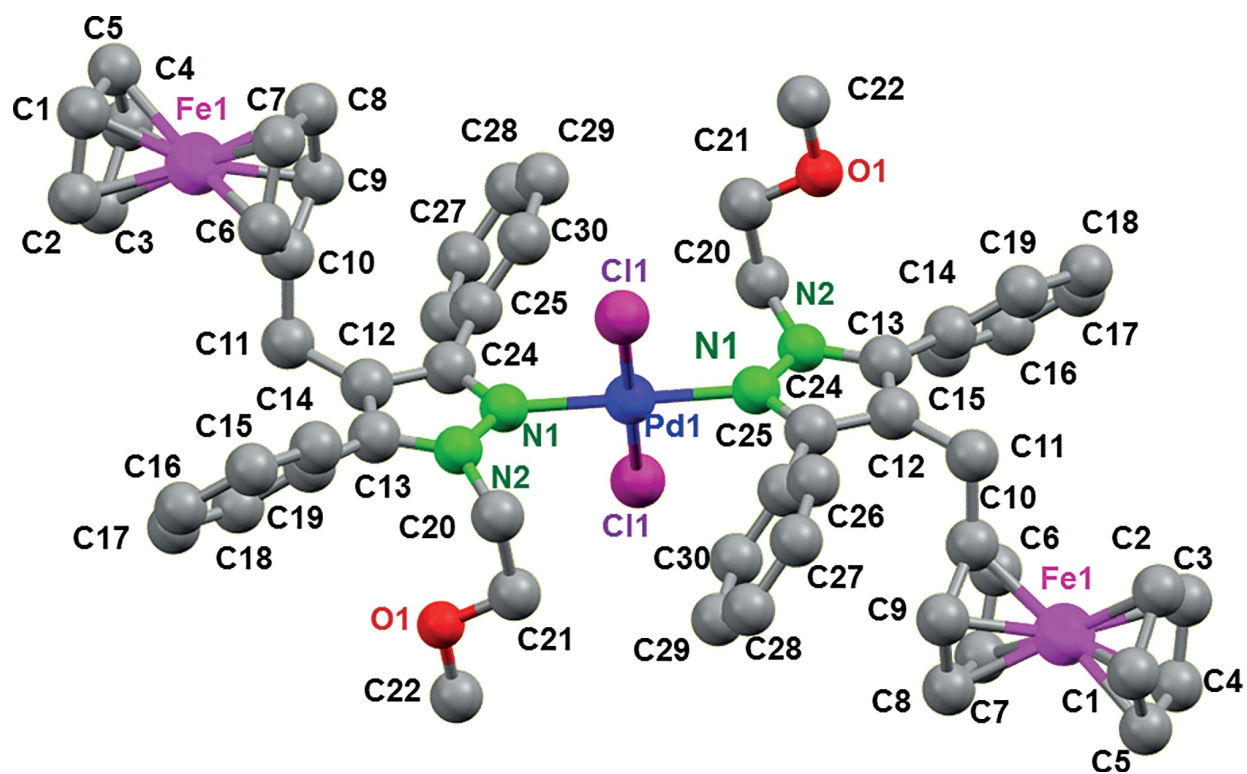
SCHEME 2.



632
633

634
635
636

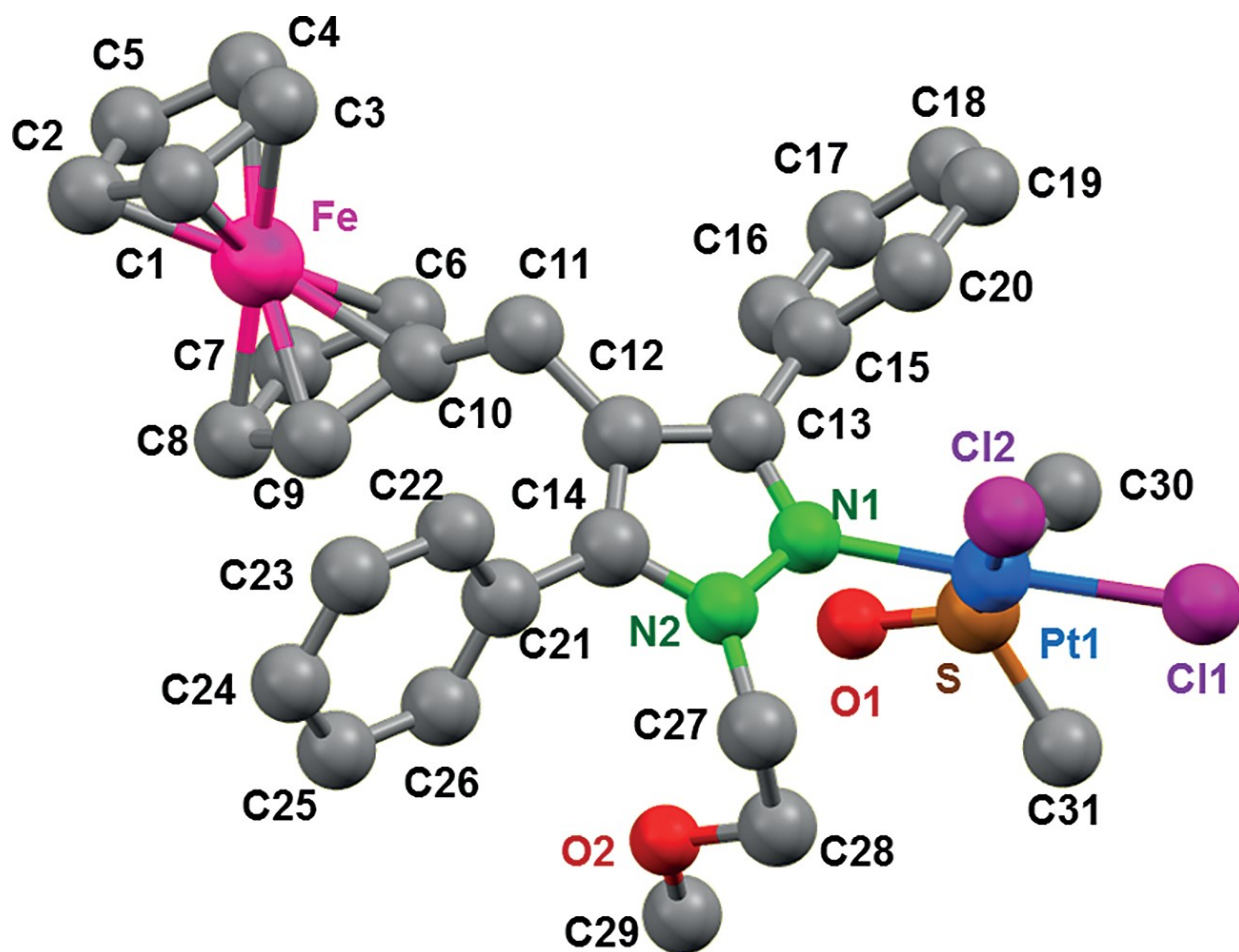
FIGURE 2.



637
638

639
640
641

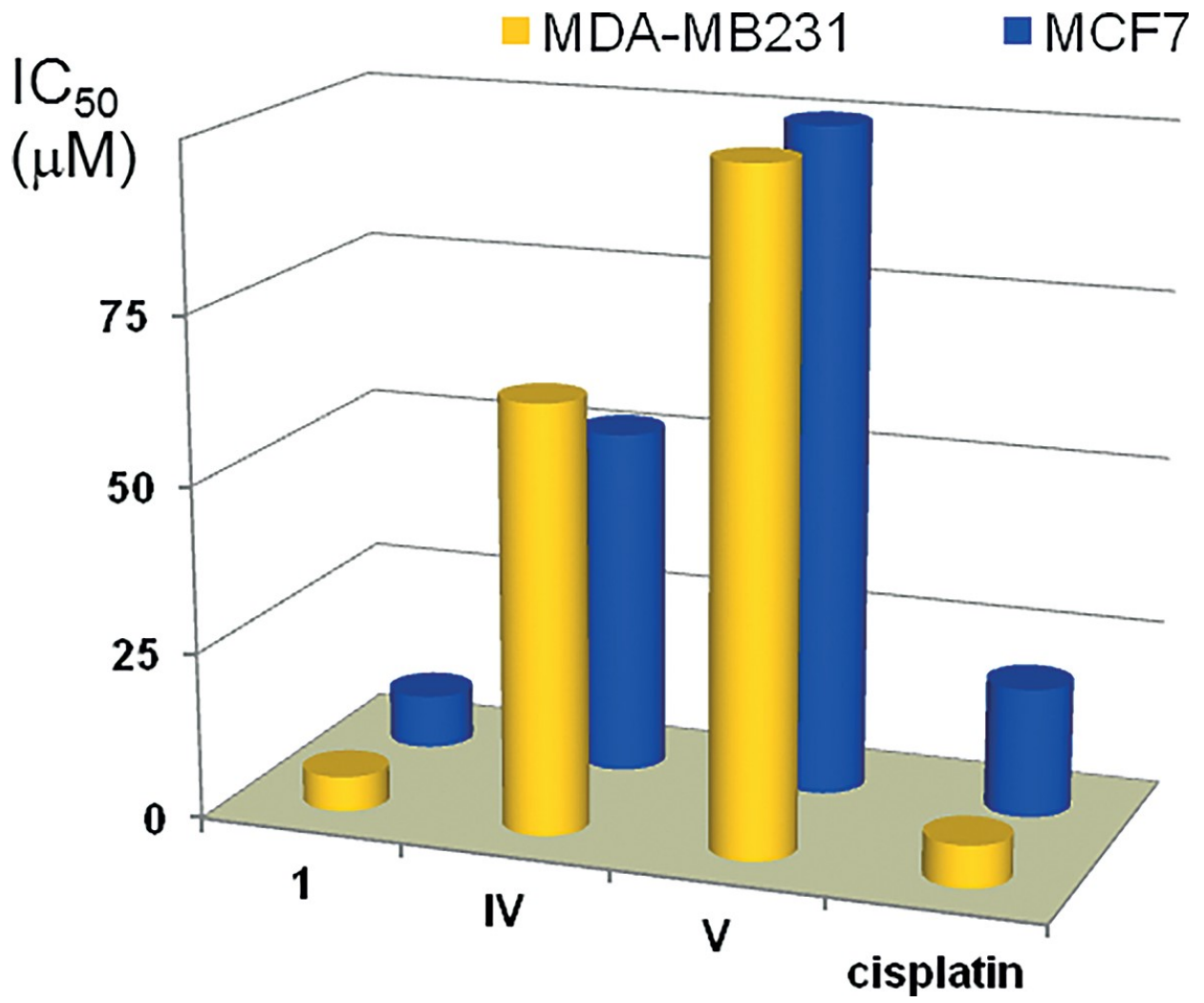
FIGURE 3.



642
643

644
645
646

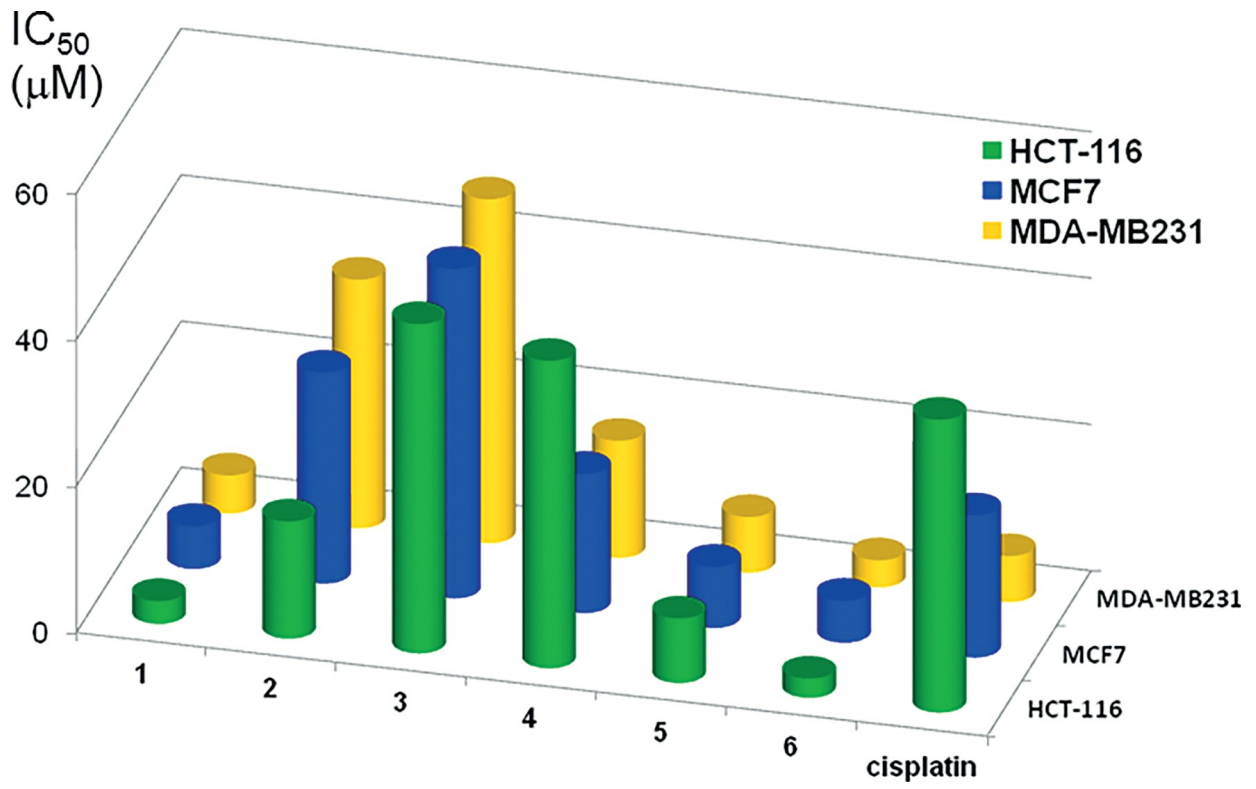
FIGURE 4.



647
648

649
650
651

FIGURE 5.



652
653
654
655

656 **Table 1.** Summary of experimental conditions [reagents, molar ratios, solvents, temperature (T) and
 657 reaction time (t)] used to prepare the new PdII complexes 2–4 (Entries 1–4) and PtII compounds 5 and 6
 658 (Entries 5 and 6). In entries 5 and 6, [Pt] represents cis-[PtCl₂(dmsO)₂]. Reagents (molar
 659

	Reagents (molar ratios)	Solvent	T	t [h]	Final products
1	1 and Na ₂ [PdCl ₄] (1:1 or 1:2)	MeOH	298 K	1	2
2	1 and [PdCl ₂ (dmsO) ₂] (1:1 or 1:2)	MeOH	reflux	1	2
3	1 and Pd(OAc) ₂	toluene	reflux	24	3
4 ^[a]	(1) 3 and LiCl ^[b]	acetone	298 K	1	
	(2) PPh ₃ ^[c]	CH ₂ Cl ₂	298 K	1	4
5	1 and [Pt]	MeOH	reflux	1	5
6	1, [Pt], and NaOAc (1:1:2)	toluene/ MeOH ^[d]	reflux	24	5 and 6 ^[e]

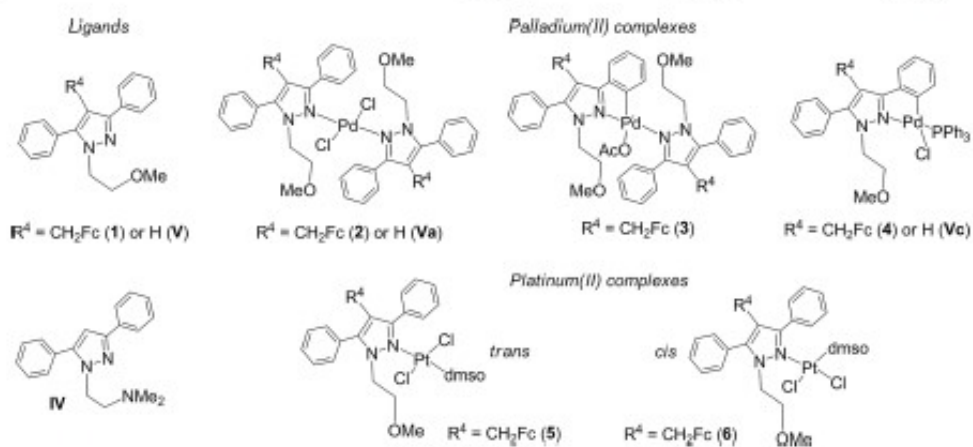
[a] Two-step sequence. [b] Molar ratio LiCl/3 = 1.5. [c] Molar ratio 3/PPh₃ = 1:1. [d] A 5:1 Mixture. [e] Molar ratio 5/6 = 1.0:3.8.

660

661

662 **Table 2** Cytotoxic activities (IC₅₀ values in μm) against breast cancer cell lines (MCF7 and MDA-
 663 MB231) and the cisplatin-resistant HCT-116 colon cell line for the pyrazoles. To ease the identification
 664 of the compounds included in this study, their chemical formulae are shown below.
 665

Compound	R ⁴	Binding mode	MCF7	MDA-MB231	HCT-116
1	CH ₂ Fc	–	5.8 ± 0.9	5.2 ± 0.7	3.1 ± 0.5
V	H	–	>100	100	[a]
IV	H	–	52 ± 10	64 ± 24	[a]
2	CH ₂ Fc	(N)	28 ± 2.3	34 ± 1.7	16 ± 3
Va	H	(N)	>100	75 ± n.d.[b]	[a]
3	CH ₂ Fc	(N) and (C,N) ⁻	45 ± 2.6	47 ± 2.8	45 ± 3.1
Vc	H	(C,N) ⁻	67 ± 1.9	13 ± 1.1	[a]
4	CH ₂ Fc	(C,N) ⁻	19.6 ± 1.7	16.1 ± 1.3	42 ± 4.3
5	CH ₂ Fc	(N)	8.3 ± 1.1	7.6 ± n.d.[b]	8.5 ± 0.9
6	CH ₂ Fc	(N)	5.7 ± 0.8	3.7 ± n.d.[b]	2.6 ± 0.6
cisplatin			19.4 ± 4.5	6.3 ± 3.4	40 ± 4.4



[a] Data not available. [b] n.d.: not determined.

666

667

668 **Table 3** Crystal data and details of the refinement of the crystal structures of 2 and 6·CH₂Cl₂·MeOH.

669

	2	6·CH ₂ Cl ₂ ·MeOH
Empirical formula	C ₃₀ H ₃₀ Cl ₂ Fe ₂ N ₄ O ₂ Pd	C ₃₀ H ₃₇ Cl ₆ FeN ₂ O ₇ PtS
Formula weight	1130.7	936.46
Crystal size [mm]	0.090 × 0.180 × 0.240	0.180 × 0.220 × 0.34
Crystal system	monoclinic	monoclinic
Space group	<i>P</i> 2 ₁ / <i>c</i>	<i>C</i> 2/ <i>c</i>
<i>a</i> [Å]	11.7349(12)	29.6708(14)
<i>b</i> [Å]	18.7496(17)	14.6180(8)
<i>c</i> [Å]	11.7367	16.4452(10)
$\alpha = \gamma$ [°]	90.0	90.0
β [°]	97.217(4)	98.887(2)
T [K]	100(2)	100(2)
λ [Å]	0.71073	0.71073
<i>V</i> [Å ³]	2561.9(4)	7047.1(7)
<i>Z</i>	2	8
<i>D</i> _{calc} [Mg/m ³]	1.465	1.795
<i>F</i> (000)	1149	3704
μ [mm ⁻¹]	1.057	4.776
θ range [°]	2.06–25.13	2.507–25.109
Collected reflections	10506	28067
Unique reflections [<i>R</i> (int)]	4519 [0.0442]	626 [0.0820]
Parameters	302	407
<i>R</i> indices [<i>I</i> > 2 σ (<i>I</i>)]	<i>R</i> ₁ = 0.0658, <i>wR</i> ₂ = 0.1545	<i>R</i> ₁ = 0.0415, <i>wR</i> ₂ = 0.1115
<i>R</i> indices (all data)	<i>R</i> ₁ = 0.1013, <i>wR</i> ₂ = 0.1762	<i>R</i> ₁ = 0.0471, <i>wR</i> ₂ = 0.1168

670

671

672